UDC 533.6.013.422 :
534.12

TECHNICAL REPORT OF NATIONAL AEROSAPCE LABORATORY

TR-315T

Natural Vibration and Panel Flutter of Cylindrically Curved Panels

Yuji MATSUZAKI

April 1973

NATIONAL AEROSPACE LABORATORY

CHŌFU, TOKYO, JAPAN

List of NAL Technical Reports

TR-290 Study of a Rotary-drive Vibratory-output Two-degree-of-freedom Gyro	Hiroshi YAMADA	July 1972
TR-291 On the Natural Vibration of Plate-Beam Conbination Structures (III)	Taketoshi HANAWA, Yoichi HAYASHI, Yasuo TADA, Susumu TODA, Kazuo KUSAKA	July 1972
TR-292 An Approximate Calculation Method of Incompressible Turbulent Wakes behind Aerofoils–Symmetrical Wake Flow Case–	Yoji ISHIDA	July 1972
TR-293 An Elastic-Plastic Analysis of a Crack with Linearly Distributed Stress in the Plastic Zone.	Hiroyuki TERADA	Aug. 1972
TR-294 Effect of Ground Proximity on the Longitudinal Aerodynamic Characteristics of an Airplane with a Jet-Flapped High Lift Wing	Hiroshi ENDO, Hiroshi TAKAHASHI, Teruomi NAKAYA, Tadaharu WATANUKI	Aug. 1972
TR-295 Orbit Determination and Control Methods for Self-Contained Station-Keeping Systems	Koichi MATSUSHIMA	Aug. 1972
TR-296 Liner Cooling of the Aeronautical Gas Turbine Combustor	Tetsuro AIBA	Aug. 1972
TR-297 A Calculation of Temperature Distribution by Applying Green's Function to a Two-Dimentional Laplace's Equations. (The Case in which the Temperature Gradients on the Boundary are Given)	Hideaki NISHIMURA, Hiroshi USUI	Aug. 1972
TR-255 T The Study on the Motion of an Artificial Satellite in the Earth's Gravitational Field	Sumio TAKEUCHI, Koichi MATSUSHIMA	Aug. 1972
TR-298 Experiment on Airspeed Calibration Procedure	Jiro KOO, Toichi OKA, Yukichi TSUKANO, Kenji YAZAWA, Koji ONO	Jan. 1973
TR-299 On the Drag Divergence of Two-Dimensional Airfoils at Transonic Speeds	Nobuhiko KAMIYA	Jan. 1973
TR-300 Experimental Investigation of Two-Dimensional Cascade Performance with Thin and Low-Cambered Double-circular Arc Blade Sections at Transonic Inlet Mach Number Range	Hajime SAKAGUCHI, Hiroshi KONDO, Susumu TAKAMORI, Keigo IWASHITA	Oct. 1972
TR-301 A Mathematical Theory on Evaluation of Observation Systems	Takeo KIMURA	Sept. 1972
TR-302 Estimation of Guidance Errors by Kalman-Bucy Filtering Technique	Masaaki MURATA	Oct. 1972
TR-303 Studies of IDPF Servovalve Appropriate for Gimbaled Engine Positioning Hydraulic Control Systems	Shigeki HATAYAMA	Nov. 1972
TR-304 Study on a Synchronizing Control of a Drag-Cup Gyro Motor	Hiroshi YAMADA	Nov. 1972
TR-305 Coordinate Transformation Algorithm by the Eulerian Angels Representation	Yoshiaki OKAMI	Nov. 1972
TR-306 System Design of Facilities for VTOL Flying Test Bed at National Aerospace Labotory	Naoto TAKIZAWA, Akiyoshi SHIBUYA, Toshio OGAWA, Hirotoshi FUJIEDA, Tadao KAI, Yoshito MIYAMOTO,	Nov. 1972

Natural Vibration and Panel Flutter of Cylindrically Curved Panels*

By Yuji MATSUZAKI**

流れに垂直な方向にのみ曲率を持つ浅い曲面板のパネルフラッタ特性に及ぼす，面内境界条件とパネルの形状の影響について調べた。複雑なパネルフラッタ特性を十分理解するためには固有振動特性を知ることが不可欠であるので，高次のモードまでの固有振動の計算も併せて行なった。REISSNER型の殻の方程式を用い，GALERKIN 法を適用して解析を行った。パネルの振動波形は二重フーリェ級数の形に仮定し，数値計算では流れの方向に最大10項まで，流れに垂直方向には2項までとった。計算結果によれば，面内境界条件とパネルの形状の影響は，従来の報告より一層複雑であることが明らかになった。ある形状のパネルでは，振動波形の仮定で流れに垂直方向に2項まで取ることによって初めて，空力弾性的に連成しやすいモードの固有振動数の一致することが示され，又その時2項まで取る解析によってのみフラッタ限界値の大幅な低下が示されることも明らかになった。これは，流れに垂直な方向に1項のみの振動波形で解析する場合には，十分な注意が必要であることを意味している。パネルフラッタ防止のためには，結論として，流れに垂直な方向にのみ曲率を持ち，縦横比が1に近い四辺単純支持の曲面板では，前，後縁で流れに垂直な方向の面内変位を拘束し，側辺では流れに垂直な方向の面内変位を拘束しないこと（垂直合力=0）が望ましい。

ABSTRACT

Influences of in-plane boundary conditions and panel geometry on natural vibration and flutter characteristics of cylindrically curved panels, exposed to a supersonic flow parallel to the generators, are analyzed with the aid of Galerkin's method within the framework of Reissner's shallow shell theory. Almost all results are obtained by using twelve assumed modes, namely, a combination of the first six streamwise and the first two symmetrical spanwise modes. Convergence of flutter solutions is checked by taking the first ten streamwise modes at the most. The numerical results have revealed that influences of in-plane boundary conditions and panel geometry are much more complicated than previously reported. Since some results indicate that spanwise modal coupling due to the in-plane edge restraint yields coincidence of natural frequencies which has a detrimental effect on flutter boundary, omission of the higher spanwise modes in flutter analysis leads to erroneous results for such cases. Although the present analysis has limitation on choice of combinations of the in-plane boundary conditions, a general recommendation for flutter prevention of curved panels whose aspect ratio is about 1 is that the panels should be able to move freely along the spanwise direction at straight edges and be tangentially restrained at curved edges. Comparison between results predicted by the quasi-steady and the steady aerodynamic theories indicates that the static aerodynamic theory would provide a good prediction for flutter of such panels.

NOMENCLATURE

a = a half of length of a panel along straight edges

b = a half of breadth of projection of a panel on x-y

* Received January 5, 1973 ** First Airframe Division

plane (see Fig. 1)
D = bending stiffness
E = Young's modulus
F = stress function
h = thickness of panel
M = Mach number
$I\ (p, r)$ = see Eq. (20)
$J_{oo}\ (p, r)$, etc. = see Eqs. (21)
N_x, N_y, N_{xy} = stress resultants
p_a = aerodynamic forces
q, Q = dynamic pressure
R = radius of curvature
u, v, w = displacements in x, y and z directions, respectively
U = velocity of free stream
w_{pr} = see Eq. (10)
x, y, z = coordinates
α_p, β_p, etc. = see Eq. (13)
$\beta = (M^2\text{-}1)^{1/2}$
γ_c = see Eq. (19)
$\lambda = a/b$
ν = Poisson's ratio
ρ = density of air
ρ_m = density of panel
ω, Ω = frequency
(p, r) = a natural mode predominated by an assumed mode w_{pr}

1. INTRODUCTION

Curved panels are fundamental structural components of high speed aircraft and rockets. However, not only flutter of curved panels but also natural vibration have not fully been investigated compared with those of flat plates or circular cylindrical sehlls since a great number of parameters are involved in the problem. In particular, little experimental data are available. In the present paper we shall restrict ourselves to cylindrical panels exposed to a supersonic flow parallel to the generators although flutter of panels with streamwise curvature is also of great importance. Since a history of analyses of natural vibration has briefly presented in Ref. 1, an outline of previous works on panel flutter will be given here.

The first theoretical investigation by Voss[2], who used the Reissner shallow shell theory and the Ackeret aerodynamic theory, showed that stiffening due to shell curvature raised considerably flutter boundary from the level of flat plates. Hess and Gibson[3] made an experiment of a cylindrical panel axially loaded to a stress near the buckling stress. The compressive stress had a large effect on flutter boundary, which appeared to attain a minimum value at the calculated buckling stress. Another experimental work by Presnell and Mckinney[4] indicated that pressure differential was strongly influential to flutter boundary and that flutter characteristics were highly dependent on the panel shape caused by the pressure differential. Bolotin[5] formulated a nonlinear problem for a plate of general curvature by taking into account the geometrical nonlinearity in von Karman's large deflection theory although no solutions were given. McElman[5] presented a formula for flutter boundary of curved sandwich panels. Another study of interest was made by Anderson and Hsu[7]. The aerodynamic forces were approximated by a static theory which included a correction parameter for pressure distribution along the flow direction. As the parameter varied, the pressure distribution changed from that given by the Ackeret theory to that of a steady, slender body theory. The numerical results showed that the critical dynamic pressure was less sensitive to the pressure distribution than previously expected.

Along the line of Bolotin's presentation, Dowell[8,9] has given a nonlinear formulation* for panels with general curvature subjected to a set of the in-plane boundary conditions S_x3 and S_y3 (See Eqs. (9) in the text) in an average sense and presented extensive numerical results. As far as panels with only spanwise curvature are concerned, a significant finding is that in-plane edge restraint has a great influence on flutter boundary. Contrary to Voss' conclusion that the spanwise curvature has a stabilizing effect, the critical dynamic pressure is found to decrease monotonically as the curvature increases. Confirming

* As well known, flutter boundary for panels with only spanwise curvature can be determined without nonlinear terms being taken in an analysis. Strictly speaking in a linear case of such panels in Ref. 8, the modes with odd number of half-waves between edges satisfy the in-plane boundary condition of zero normal displacement on an average, but the modes with even number of half-waves identically satisfy the in-plane boundary condition S_x2 or S_y2 in an exact sense. This inconsistency of the in-plane edge restraint may mislead to coincidence of frequencies of the first two streamwise modes which is reported in Ref. 9.

that Voss' result is true for the set of the conditions S_x2 and S_y2, Dowell has pointed out in Ref. 10 as follows: for in-plane boundary condition of zero normal displacement the stiffening due to spanwise curvature is selective and the frequency of the streamwise fundamental mode is raised to a greater degree than that of the second. Hence, the frequency (squared) difference is decreased and flutter is more likely. Recently Salvioni[11] has performed nonlinear flutter analysis of buckled and unbuckled cylindrical panels subjected to axial compressive loads with the aid of graphic presentation.

As for natural vibration of cylindrical panels the present author[1] has recently shown by using the two-mode Galerkin procedure that in-plane boundary conditions have a great effect on natural vibration characteristics. In the present paper, therefore, effect of the in-plane boundary conditions as well as that of panel geometry on flutter characteristics will be studied by using the two-dimensional quasi-steady aerodynamic theory within the framework of Reissner's shallow shell theory. The natural vibration characteristics in the higher mode approximation, which are calculated by setting the dynamic pressure equal to zero in the flutter analysis, will be also presented. The same approach as in Ref. 1 shall be taken in which a homogeneous solution of stress function is expressed in terms of trigonometric and hyperbolic functions so that several sets of the in-plane boundary conditions can be exactly satisfied. As a consequence of employing the quasi-steady aerodynamic forces, a coupled type of flutter is only one possible instability and occurs due to coalescence or closeness of frequencies of the aeroelastically associated modes as the dynamic pressure increases. Hence, it is quite instructive to investigate the natural frequency characteristics in order to get a better understanding of complicated features of flutter.

Although several numbers of calculations for spanwisely antisymmetrical modes have been carried out, we will here focus on results for the spanwisely symmetrical modes. Almost all results are obtained by using twelve assumed modes, namely, a combination of the first six streamwise and the first two symmetrical spanwise modes. Convergence of flutter solutions solved with the aid of the Galerkin method is checked by employing the first ten streamwise modes at the most. Comparison is made between flutter characteristics determined by using the quasi-steady and the static aerodynamic theories.

There are no experimental data known to the author which provide a proper comparison with results of the present study. In addition, a large amount of computation time is required in order to cast a spotlight thoroughly on several problems unresolved even within the framework of the present analysis. Hence, instead of presenting a general flutter boundary for design, we will give some fundamental results on specific panel configurations and flow state selected for an experiment which would be made by using the Supersonic Wind Tunnel at National Aerospace Laboratory. Radius of curvature is selected as a parameter. All of the results presented here will be for zero in-plane loading and zero pressure differential.

2. PROBLEM FORMULATION

The coordinate system, the flow direction and panel geometry defined as

$$Z(x, y)=\frac{b^2-y^2}{2R} \tag{1}$$

are illustrated in Fig. 1. The Reissner type equations of equilibrium and compatibility in the linear theory[12] are

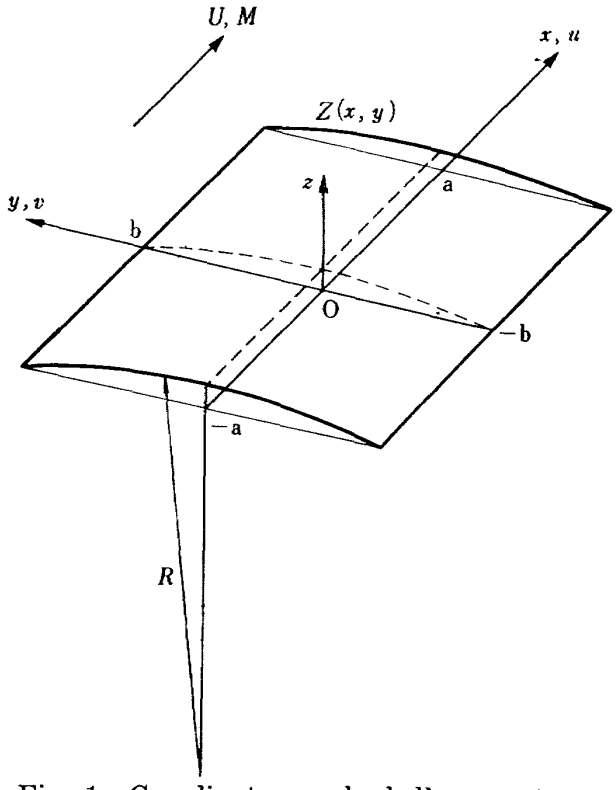

Fig. 1 Coordinates and shell geometry.

$$D\Delta\Delta w-h\frac{\partial^2F}{\partial y^2}\frac{\partial^2Z}{\partial x^2}-h\frac{\partial^2F}{\partial x^2}\frac{\partial^2Z}{\partial y^2}+2h\frac{\partial^2F}{\partial x\,\partial y}\frac{\partial^2Z}{\partial x\,\partial y}+\rho_m h\frac{\partial^2w}{\partial t^2}+p_a=0 \tag{2}$$

$$\Delta\Delta F=E\left[2\frac{\partial^2Z}{\partial x\,\partial y}\frac{\partial^2w}{\partial x\,\partial y}-\frac{\partial^2Z}{\partial y^2}\frac{\partial^2w}{\partial x^2}-\frac{\partial^2Z}{\partial x^2}\frac{\partial^2w}{\partial y^2}\right] \tag{3}$$

where D, E and F are bending stiffness, Young's modulus and stress function defined as

$$\frac{\partial^2F}{\partial y^2}=\frac{N_x}{h},\quad \frac{\partial^2F}{\partial x^2}=\frac{N_y}{h},\quad \frac{\partial^2F}{\partial x\,\partial y}=-\frac{N_{xy}}{h} \tag{4}$$

The aerodynamic forces p_a are approximated by the two-dimensional quasi-steady theory:

$$p_a=\frac{2q}{\beta}\left[\frac{\partial w}{\partial x}+\frac{M^2-2}{M^2-1}\frac{1}{U}\frac{\partial w}{\partial t}\right] \tag{5}$$

where

$$q=\frac{1}{2}\rho U^2 \tag{6}$$

$$\beta=(M^2-1)^{1/2} \tag{7}$$

For a panel with simply supported edges the boundary conditions to be satisfied by w are

$$w=\frac{\partial^2w}{\partial x^2}=0 \qquad \text{at } x=-a \text{ and } a \tag{8.1}$$

$$w=\frac{\partial^2w}{\partial y^2}=0 \qquad \text{at } y=-b \text{ and } b. \tag{8.2}$$

The following sets of the in-plane boundary conditions which are the same at the opposite sides of edges are considered:

$$\begin{cases} S_x1: & u=v=0 \\ \text{or } S_x2: & N_x=v=0 \\ \text{or } S_x3: & u=N_{xy}=0 \\ \text{or } S_x4: & N_x=N_{xy}=0 \end{cases} \quad \text{at } x=-a \text{ and } a, \tag{9.1}$$

$$\begin{cases} S_y1: & v=u=0 \\ \text{or } S_y2: & N_y=u=0 \\ \text{or } S_y3: & v=N_{xy}=0 \\ \text{or } S_y4: & N_y=N_{xy}=0 \end{cases} \quad \text{at } y=-b \text{ and } b. \tag{9.2}$$

For a spanwisely symmetrical case the deflection is assumed so as to satisfy Eqs. (8) as follows:

$$w=\sum_{\substack{l=1\\ l:\text{ odd}}}^{L}\sum_{\substack{n=1\\ n:\text{ odd}}}^{N} w_{ln}\cos\frac{l\pi}{2a}x\cos\frac{n\pi}{2b}y$$

$$+\sum_{\substack{m=2\\ m:\text{ even}}}^{M}\sum_{\substack{n=1\\ n:\text{ odd}}}^{N} w_{mn}\sin\frac{m\pi}{2a}x\cos\frac{n\pi}{2b}y \tag{10}$$

Substitution of Eqs. (10) and (1) into Eq. (3) yields a solution of stress function as

$$F=F_p+F_h \tag{11}$$

where F_p and F_h are particular and homogeneous solutions, respectively and

$$F_p=-\sum_l\sum_n\frac{E}{R}w_{ln}\left(\frac{2a}{\pi}\right)^2\frac{l^2}{(l^2+\lambda^2n^2)^2}\cos\frac{l\pi}{2a}x\cos\frac{n\pi}{2b}y-\sum_m\sum_n\frac{E}{R}w_{mn}\left(\frac{2a}{\pi}\right)^2\frac{m^2}{(m^2+\lambda^2n^2)^2}\sin\frac{m\pi}{2a}x\cos\frac{n\pi}{2b}y \tag{12}$$

$$F_h=\frac{E}{R}\left[\sum_l\cos\frac{l\pi}{2a}x\left(\alpha_l\cosh\frac{l\pi}{2a}y+\beta_l\frac{l\pi}{2a}y\sinh\frac{l\pi}{2a}y\right)+\sum_n\cos\frac{n\pi}{2b}y\left(\gamma_n\cosh\frac{n\pi}{2b}x+\delta_n\frac{n\pi}{2b}x\sinh\frac{n\pi}{2b}x\right)+\sum_m\sin\frac{m\pi}{2a}x\left(\alpha'_m\cosh\frac{m\pi}{2a}y+\beta'_m\frac{m\pi}{2a}y\sinh\frac{m\pi}{2a}y\right)+\sum_n\cos\frac{n\pi}{2b}y\left(\gamma'_n\sinh\frac{n\pi}{2b}x+\delta'_n\frac{n\pi}{2b}x\cosh\frac{n\pi}{2b}x\right)\right] \tag{13}$$

$$\lambda=\frac{a}{b} \tag{14}$$

Eqs. (1), (5), (10) and (11) are substituted into the left-hand side of Eq. (2) and the Galerkin procedure is used to obtain the following algebraic equations:

$$[I(p,r)+i\gamma_c\Omega-\Omega^2]\overline{w}_{pr}+J_{oo}(p,r)+2Q\sum_{\substack{m=2\\ m:\text{ even}}}\overline{w}_{mr}m\left[\frac{1}{m+p}\sin\frac{m+p}{2}\pi+\frac{1}{m-p}\sin\frac{m-p}{2}\pi\right]=0 \tag{15.1}$$
$$(p=1,3,5,\ldots;\ r=1,3,5,\ldots)$$

$$[I(q,r)+i\gamma_c\Omega-\Omega^2]\overline{w}_{qr}+J_{eo}(q,r)-2Q\sum_{\substack{l=1\\ l:\text{ odd}}}\overline{w}_{lr}l\left[\frac{1}{l-q}\sin\frac{l-q}{2}\pi-\frac{1}{l+q}\sin\frac{l+q}{2}\pi\right]=0 \tag{15.2}$$
$$(q=2,4,6,\ldots;\ r=1,3,5,\ldots)$$

where

$$w_{ln}=\overline{w}_{ln}\exp(i\omega t) \tag{16}$$

$$Q=\frac{2q}{\beta}\frac{(2a)^3}{D\pi^4} \tag{17}$$

$$\Omega=\omega\Big/\left[\left(\frac{\pi}{2a}\right)^2\left(\frac{D}{\rho_m h}\right)^{1/2}\right] \tag{18}$$

$$\gamma_c=\frac{M^2-2}{M^2-1}\left(\frac{2a\rho Q}{h\rho_m\beta}\right)^{1/2} \tag{19}$$

$$I(p,r)=(p^2+\lambda^2r^2)^2+\frac{12(1-\nu^2)}{h^2R^2}\left(\frac{2a}{\pi}\right)^4\frac{p^4}{(p^2+\lambda^2r^2)^2} \tag{20}$$

$$\begin{aligned}J_{oo}(p,r)=&-\frac{24(1-\nu^2)}{abh^2R^2}\left(\frac{2a}{\pi}\right)^4\frac{\lambda pr}{p^2+\lambda^2r^2}\\&\times\left[\frac{p\pi}{2}\sin\frac{r\pi}{2}\left\{\alpha_p\cosh\frac{p\pi}{2\lambda}\right.\right.\\&\left.+\beta_p\left(\frac{p\pi}{2\lambda}\sinh\frac{p\pi}{2\lambda}-\frac{2p^2\cosh(p\pi/2\lambda)}{p^2+\lambda^2r^2}\right)\right\}\\&-\frac{r\pi}{2}\sin\frac{p\pi}{2}\left\{\gamma_r\cosh\frac{r\pi}{2}\lambda\right.\\&\left.\left.+\delta_r\left(\frac{r\pi}{2}\lambda\sinh\frac{r\pi}{2}\lambda+\frac{2p^2\cosh(r\pi\lambda/2)}{p^2+\lambda^2r^2}\right)\right\}\right]\end{aligned} \tag{21.1}$$

$$\begin{aligned}J_{eo}(q,r)=&-\frac{24(1-\nu^2)}{abh^2R^2}\left(\frac{2a}{\pi}\right)^4\frac{\lambda qr}{q^2+\lambda^2r^2}\\&\times\left[\frac{q\pi}{2}\sin\frac{r\pi}{2}\left\{\alpha'_q\cosh\frac{q\pi}{2\lambda}\right.\right.\\&\left.+\beta'_q\left(\frac{q\pi}{2\lambda}\sinh\frac{q\pi}{2\lambda}-\frac{2q^2\cosh(q\pi/2\lambda)}{q^2+\lambda^2r^2}\right)\right\}\\&+\frac{r\pi}{2}\cos\frac{q\pi}{2}\left\{\gamma'_r\sinh\frac{r\pi}{2}\lambda\right.\\&\left.\left.+\delta'_r\left(\frac{r\pi}{2}\lambda\cosh\frac{r\pi}{2}\lambda+\frac{2q^2\sinh(r\pi\lambda/2)}{q^2+\lambda^2r^2}\right)\right\}\right]\end{aligned} \tag{21.2}$$

Unkown quantities α_p's, β_p's etc. are determined corresponding to the combination of the in-plane boundary conditions (9.1) and (9.2) as shown in Ref. 1.

For the case of natural vibration, namely, $Q=0$, Eqs. (15.1) and (15.2) are not coupled. The former represent the modal equations with respect to the streamwisely symmetrical modes and the latter the antisymmetrical modes. However, the symmetrical or the antisymmetrical assumed modes are generally coupled in the modal equations as shown in Ref. 1. Hence, each symmetrical or antisymmetrical natural mode is a general combination of the symmetrical or the antisymmetrical assumed modes, respectively. Since the α_p's, the β_p's, the α'_q's and the β'_q's (or the γ_r's, the δ_r's, the γ'_r's and the δ'_r's) vanish for the case of the inplane boundary condition S_y2 (or S_x2), the assumed modes are uncoupled and each assumed mode represents a natural mode for the combination of the conditions S_x2 and S_y2.

For the natural vibration of streamwisely symmetrical modes, the possible combinations of the in-plane boundary conditions in the present analysis are as follows:

S_x1: S_y2
S_x2: S_y1, S_y2, S_y3, S_y4
S_x3: S_y2
S_x4: S_y2

For the antisymmetrical natural vibration the following five combinations can be chosen as

S_x2: S_y1, S_y2, S_y3, S_y4
S_x4: S_y2

As for the case of flutter, namely, $Q\neq 0$ Eqs. (15.1) and (15.2) are coupled due to the aerodynamic terms and can be solved under the same five combinations of the conditions as for the antisymmetrical natural vibration.

When the determinant of the coefficients with respect to the modal amplitudes in Eqs. (15) is set equal to zero, a characteristic equation in Ω is obtained. In the flutter analysis panels are defined as unstable when the characteristic equation has at least one root with negative imaginary part.

3. NUMERICAL RESULTS AND DISCUSSIONS

Numerical calculations are carried out by employing the first two spanwise terms, namely $N=3$, in Eq. (10) since the spanwise modal coupling due to in-plane edge conditions has been demonstrated by the author[1] to have a significant influence on vibration characteristics.

3.1 Natural vibration characteristics

Although every assumed mode represents a natural mode when panels are subjected to the set of the in-plane boundary conditions S_x2 and S_y2, a natural mode is generally expressed in terms of a combination of assumed modes. Hence, let us introduce the notation (p,r) which indicates a natural mode predominated by an assumed mode of p and r half-waves in x and y directions, respectively. Since, as shown in Ref. 1, in-plane boundary conditions at straight edges are generally more influential to the natural vibration characteristics than those at curved edges, we will begin to examine the effect of the former.

Natural frequencies of the first four streamwise modes are plotted vs. R/h by solid lines in Figs. 2a, 2b, 3a and 3b although results of the first ten modes have been obtained. In

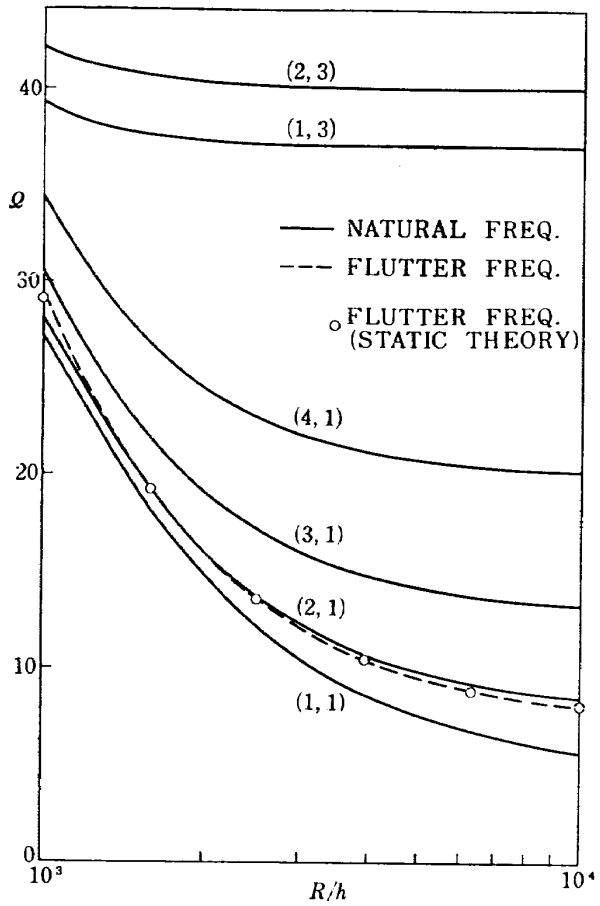

Fig. 2a Natural and flutter frequencies for $\lambda = 2$ with the conditions S_x2 and S_y1 $(2a/h = 300)$.

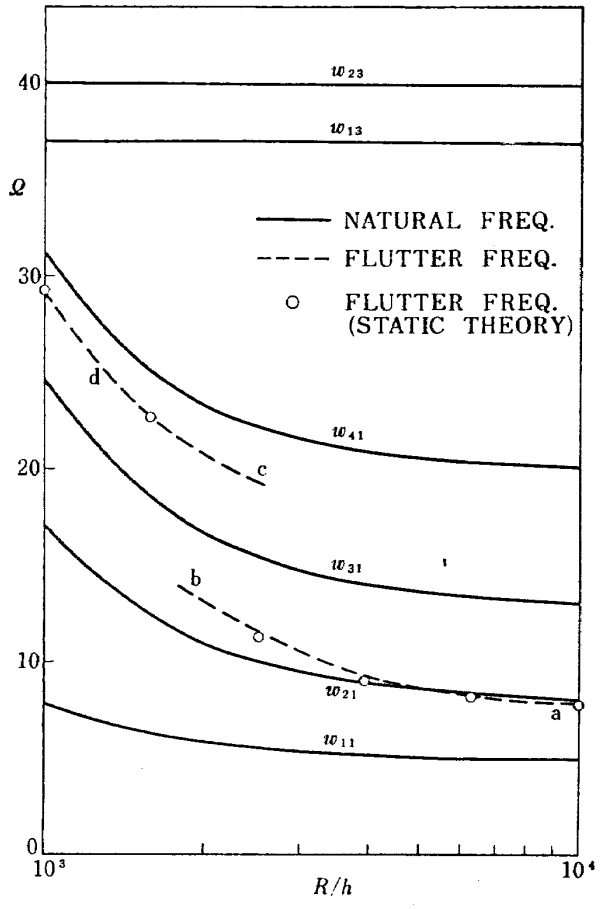

Fig. 2b Natural and flutter frequencies for $\lambda = 2$ with the conditions S_x2 and S_y2 $(2a/h = 300)$.

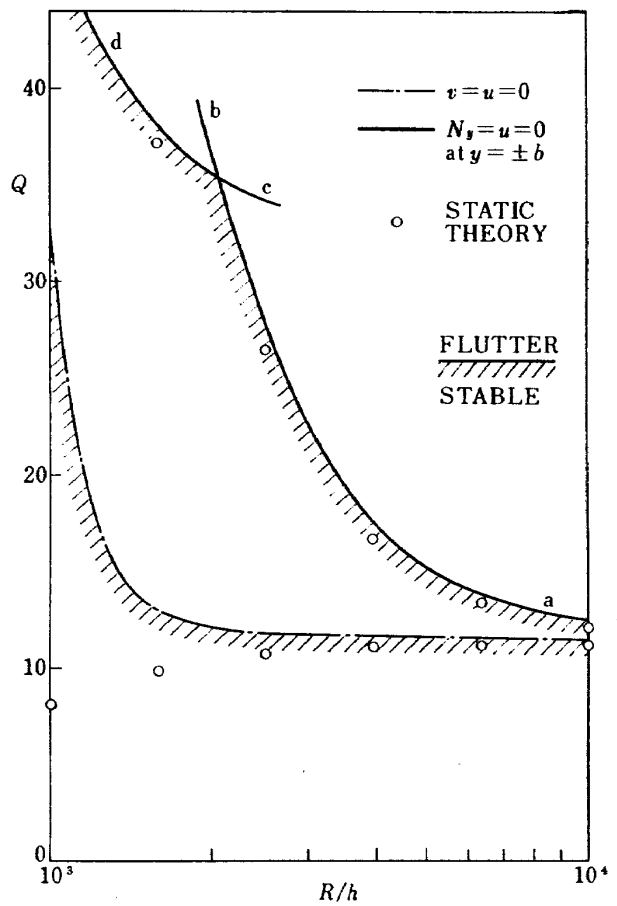

Fig. 2c Flutter boundary for $\lambda = 2$ with the combination of S_x2.

Figs. 2a and 2b we present results for panels of $\lambda = 2$ and $2a/h = 300$ subjected to the conditions S_y1 and S_y2, respectively, with the combination of the condition S_x2 at $x = \pm a$. Indeed, the figures provide a typical comparison between the effects of conditions of zero normal displacement and zero normal stress on natural frequency. Since restraint of zero displacement stiffens panels, the frequency of panels with the restraint is increased from the frequency level of panels without the restraint. The lower the mode, the greater the rate of increaes in frequency. It should be noted that the increasing rate of the streamwisely lower and spanwisely fundamental modes, namely the (1, 1) and the (2, 1) modes, becomes significantly high with increasing curvature. According to numerical results, qualitative features of frequency spectrum of panels for the condition S_y3 or S_y4 are quite similar to those for the condition S_y1 or S_y2, respectively. The quantitative comparison of the lower modes are given in Ref. 1.

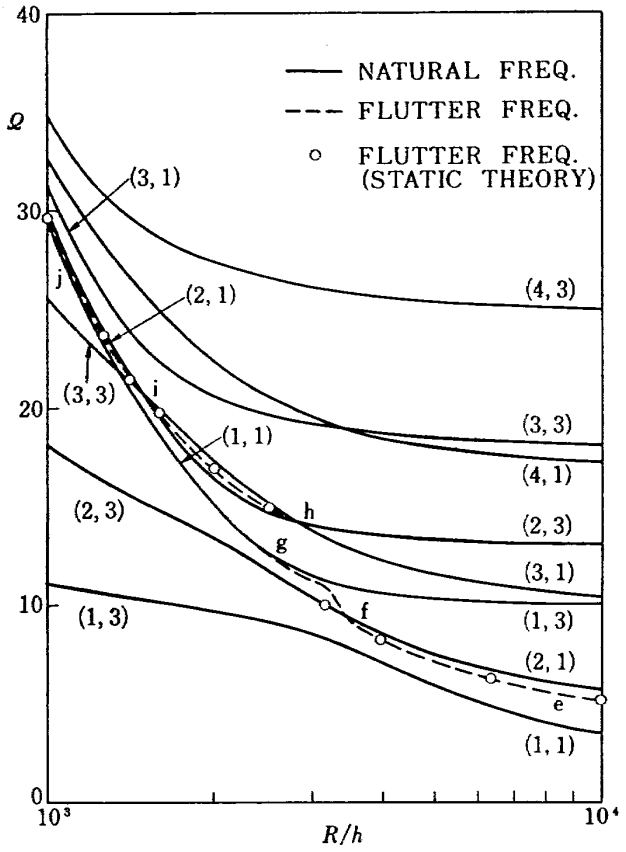

Fig. 3a Natural and flutter frequencies for $\lambda = 1$ with the conditions S_x2 and S_y1 $(2a/h = 300)$.

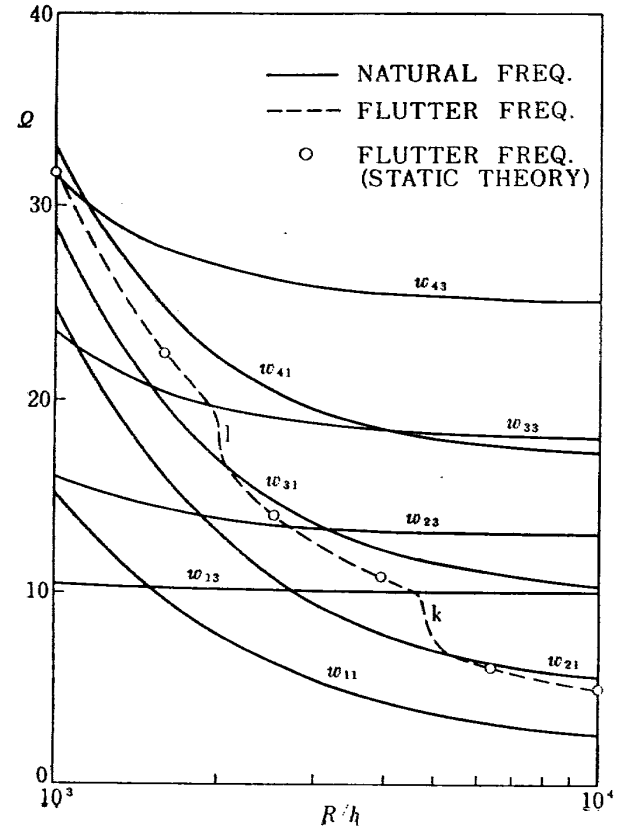

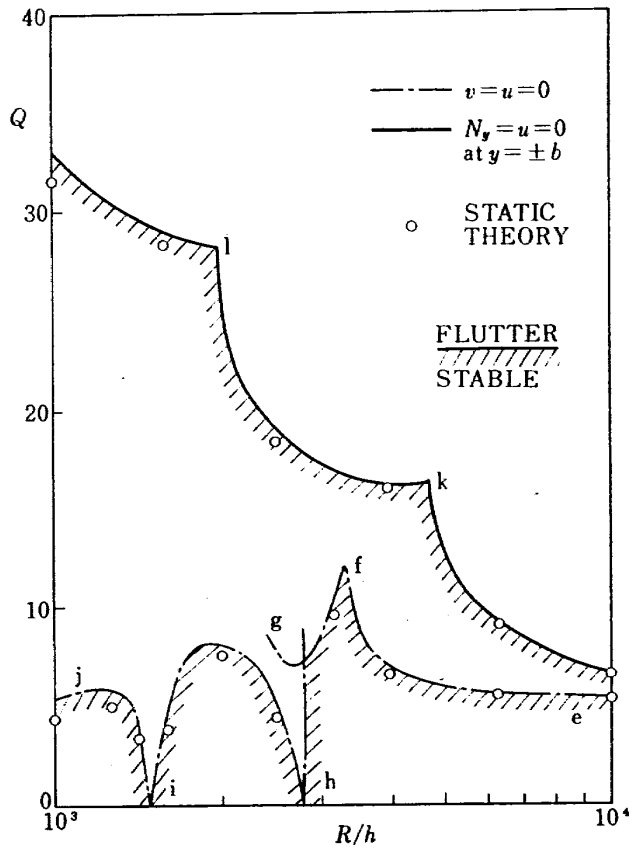

Fig. 3c Flutter boundary for $\lambda = 1$ with the combination of S_x2.

In Figs. 3 we compare results for panels of $\lambda = 1$ and $2a/h = 300$ subjected to the set of the conditions S_x2 and S_y1 with those for the conditions S_x2 and S_y2. Since frequency curves of the spanwisely lower and the spanwisely higher modes intersect in the curvature range presented, frequency spectra in Figs. 3a and 3b become much more complicated than those in Figs. 2a and 2b. In particular, Fig. 3a presents a typical illustration that each natural mode is a combination of w_{p1} and w_{p3} $(p = 1,2,..)$, for example $p = 1$, with the lower natural frequency mode being predominately w_{11} for large R/h and w_{13} for small R/h. On the contrary, the higher frequency mode is predominately w_{13} for large R/h and w_{11} for small R/h. It may be concluded from comparison between the corresponding frequency spectra that influences of in-plane boundary conditions and curvature are basically the same for panels of $\lambda = 1$ as for those of $\lambda = 2$.

Fig. 3b Natural and flutter frequencies for $\lambda = 1$ with the conditions S_x2 and S_y2 $(2a/h = 300)$.

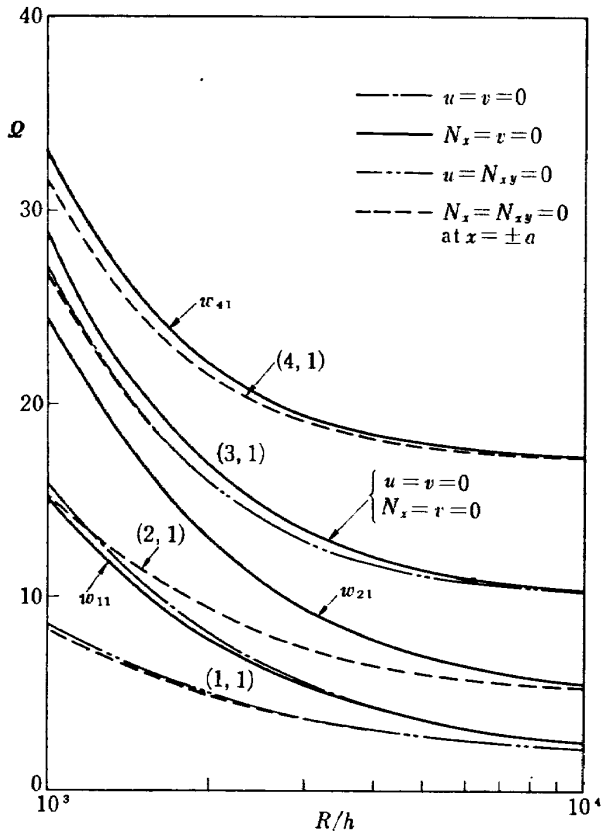

Fig. 4a Natural frequency for $\lambda = 1$ with the combination of S_y2 ($2a/h = 300$).

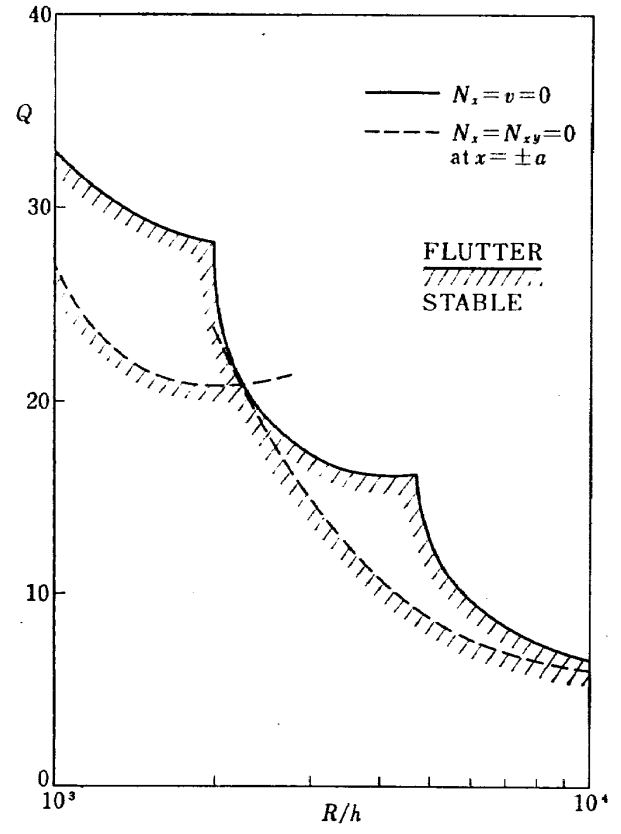

Fig. 4b Flutter boundary for $\lambda = 1$ with the combination of S_y2.

Figure 4a demonstrates the effects of the in-plane boundary conditions at $x = \pm a$ on natural frequencies of spanwisely fundamental modes for panels of $\lambda = 1$. The frequency of panels constrained by the condition S_x1, S_x2, S_x3 or S_x4 with the combination of the condition S_y2 is indicated by chain, solid, faint or broken lines, respectively. Natural frequency of streamwisely antisymmetrical modes of panels subjected to the condition S_x1 or S_x3 cannot be calculated by the present analysis as shown in § 2. What differ from the results presented in Figs. 3a and 3b are that the tangential in-plane conditions are more influential than the normal conditions and that the tangential restraint gives more restrictions to the panels rather than the normal one. It depends on the aspect ratio whether the tangential or the normal restraint is more effective. The in-plane edge conditions at curved edges become less influential with increasing aspec ratio.

3.2 Flutter characteristics

Results are presented for shells mounted in a blowdown type wind tunnel in which a flow may be assumed to be isentropic. The assumption of such a flow gives[13]

$$\rho = \frac{2q}{M^2\gamma^* R^* T_0}\left(1+\frac{\gamma^*-1}{2}M^2\right) \qquad (22)$$

where γ^*, R^* and T_0 represent the specific heat ratio ($= 1.4$), the gas constant ($= 2.868 \times 10^8$ mm^2/sec^2 °K) and the temparature of gas in a resovior, respectively. Shell properties and flow conditions used in the calculations are as follows:

$$\begin{aligned} &a=150^{mm},\ h=1^{mm},\ \lambda=1 \text{ and } 2,\ \nu=0.25,\\ &\rho_m=0.813\times10^{-9}\text{kg sec}^2/\text{mm}^4,\\ &E=1.28\times10^4\text{kg/mm}^2,\ M=2,\ T_0=300°\text{K} \end{aligned} \qquad (23)$$

The radius of curvature is selected as a parameter.

In Figs. 2c and 3c, we compare flutter boundaries of panels subjected to the in-plane boundary conditions S_y1 and S_y2 at $y = \pm b$, which are illustrated by chain and solid lines, respectively. The corresponding flutter frequencies are plotted by broken lines in Figs. 2a, 2b, 3a and 3b. As can be seen in Fig. 2c, curvature has not a destabilizing effect for panels of $\lambda = 2$. It should be noted that the flutter boundary of panels with the normal restraint at straight edges is significantly lower than that of panels without the restraint

over the range of curvature studied. In the present analysis no attempt for determination of flutter mode is made. However, Fig. 2a suggests that the panels restrained become unstable due to predominant coupling of the first two streamwise modes with a single spanwise half wave. On the other hand, it may follow from Fig. 2b that the flutter mode of the unrestrained panels predominantly consists of the first two streamwise modes for large R/h and the 3rd and the 4th for small R/h.

For panels of $\lambda = 1$, Fig. 3c also illustrates that flutter boundary of panels without the restraint increases with increasing curvature. Although the flutter boundary has a similar form to that of $\lambda = 2$, Fig. 3b implies that the predominant streamwise modes in aeroelastic coupling are the first two ones in a lower range of curvature, the 2nd and the 3rd in a moderate range and the 3rd and the 4th in a higher range. The transitions of the predominant modes take place gradually near the points k and l. On the other hand, Figs. 2b and 2c indicate that the predominant modes of panels of $\lambda = 2$ change instantaneously at the point where the flutter boundaries ab and cd cross.

As for the spanwisely restrained panels of $\lambda = 1$, the most striking feature is that the flutter boundary has peaks and abrupt drop-offs to zero.* In Fig. 3a we can easily find explanations for the unexpected flutter boundary. Firstly, the flutter frequency curve efg suggests that the assumed modes w_{11} and w_{21} are predominant in the flutter modes. Since near the point f predominancy of the w_{11} mode passes from the lower natural frequency mode into the higher frequency mode, the flutter boundary is not monotonous and may be expected to have a peak at the point f. Secondly, it is noted that over the portions, between intersecting points h and i, of two natural frequency curves the share of the w_{21} or the w_{31} mode in each natural mode is not small. Hence, frequency coincidence of such natural modes may be expected to have a detrimental influence on flutter boundary. Since the spanwise modal coupling due to in-plane edge restraint yields these frequency coincidences, omission of the spanwisely higher modes may lead to erroneous results for such panels. In fact, numerical results of the analysis without the higher modes indicate that the flutter boundary is of similar form to that for the condition S_y1 in Fig. 2c. Contrary to the results of the spanwisely two-mode approximation curvature has not a destabilizing effect at all. Lastly, as curvature is increased further, the first two streamwise modes are predominantly coupled to flutter again. As for panels subjected to the set of the conditions S_x2 and S_y3, numerical results indicate that flutter boundary which corresponds to the portion ij in Fig. 3c has a steep ascent and no peaks although there is little difference between the natural frequency spectra for the conditions S_y1 and S_y3 with the combination of the condition S_x2. Both critical dynamic pressure at $R/h = 1000$ shall be compared in Fig. 6.

Since, as shown in §§ 3.1, natural frequency for $\lambda = 1$ is more sensitive to the tangential conditions at curved edges than to the normal conditions, in Fig. 4b we shall present flutter boundary for the panels subjected to the in-plane boundary conditions S_x2 and S_x4 with the combination of the condition S_y2 at $y = \pm b$. We note that the flutter boundary is so much dependent on the tangential conditions at curved edges and that the tangential constraint has a stabilizing effect.

It can be concluded from the results discussed above that the flutter characteristics are strongly affected by the in-plane boundary conditions and the panel geometry. The results have revealed that the effect of the in-plane boundary conditions are much more complicated than reported by Dowell.

In order to examine convergence of flutter solutions solved with the aid of Galerkin's method, Figs. 5 and 6 illustrate flutter boundary vs. streamwise modes for panels of $R/h = 1000$ and ∞ i.e., flat plates. For the curved panels an open or a solid symbol indicates that flutter is predicted as predominant coupling of the first two streamwise assumed modes or the 3rd and the 4th, respectively. As far as the first two modes are predominantly coupled, the critical dynamic pressure which is predicted by using the first six or eight assumed modes is within about five percent of the converged value. However, the higher approximation is required to get a satisfactory prediction of flutter caused by coupling of the higher streamwise modes.

* When frequencies of natural modes coincide which play important roles in an aeroelastic coupling, employment of the assumption of an isentropic flow leads to prediction of zero critical dynamic pressure even if aerodynamic damping exists. See Appendix.

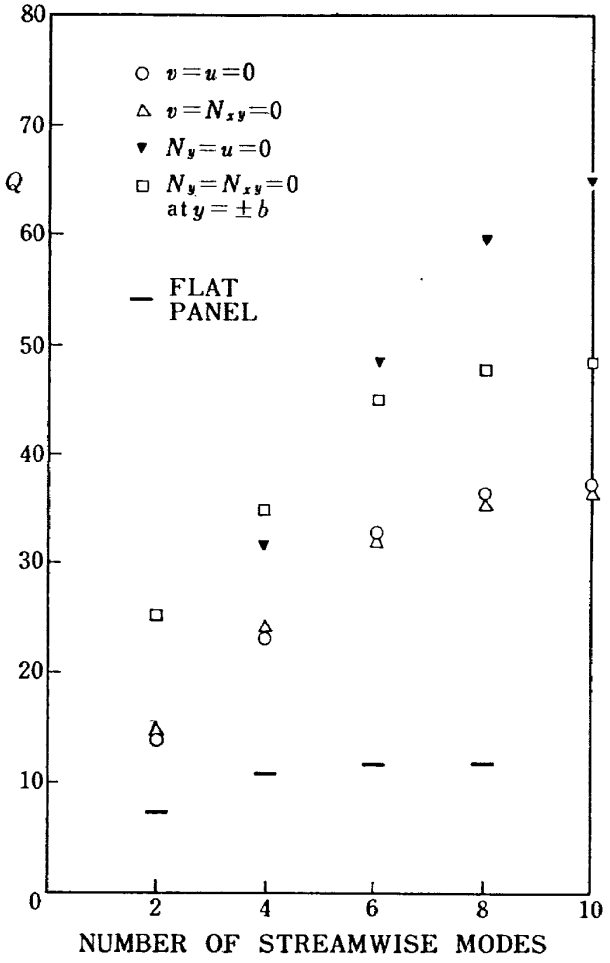

Fig. 5 Flutter boundary for $\lambda=2$ and $R/h=1000$ with the combination of S_x2.

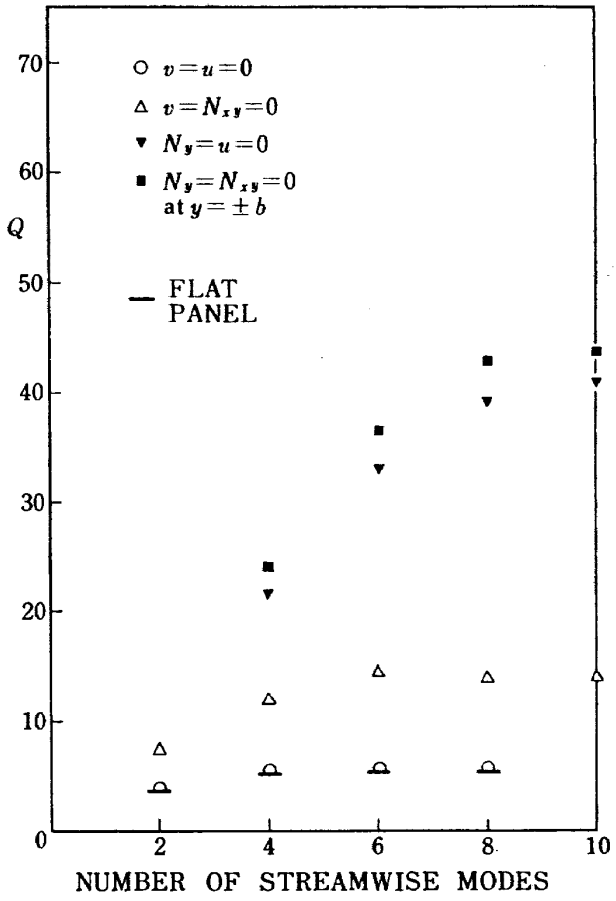

Fig. 6 Flutter boundary for $\lambda=1$ and $R/h=1000$ with the combination of S_x2.

Consequently, it may be anticipated in Fig. 2c and 3c that the portion of the flutter boundary predicted as predominant coupling of higher streamwise modes will be shifted upwards by the higher approximation. Generally speaking, curved panels with the normal constraint at straight edges need fewer streamwise assumed modes for convergence of solutions than the panels without the constraint. Figs. 5 and 6 also prove that the in-plane boundary conditions have a great influence on the flutter characteristics.

So far we have discussed numerical results, for specific panels and flow, calculated by using the quasi-steady aerodynamic theory. Lastly, we will assume no aerodynamic damping, i.e., $\gamma_c=0$ in Eqs. (15) in order to study effect of aerodynamic damping. Let us return to Figs. 2 and 3. Open circles represent the flutter frequency and the critial dynamic pressure predicted by the static aerodynamic theory. It should be noted that the flutter characteristics determined by using the static theory agree well with those by the quasi-steady theory except for panels of $\lambda=2$ with the normal restraint at $y=\pm b$ for small R/h. As far as they are expected to agree, the results presented here by using the quasi-steady theory may be applicable to more general panel configurations and flow condition, since the static aerodynamic theory needs fewer parameters in the analysis.

4. CONCLUSIONS

Influences of panel geometry and in-plane boundary conditions on natural vibration and flutter characteristics of cylindrically curved panels have been analyzed with the aid of Galerkin's method within the framework of Reissner's shallow shell theory.

Numerical results indicate that both characteristics are greatly affected by in-plane boundary conditions and panel geometry and that the influences are much more complicated than reported in Ref. 9. Since some results demonstrate that spanwise modal coupling due to in-plane boundary restraint yields the frequency coincidence of aeroelastically asso-

ciated modes which has a detrimental effect on flutter boundary, it is quite essential to include the higher spanwise assumed modes in flutter analysis of such panels.

Although the present analysis has limitation on choice of combinations of in-plane boundary conditions, a general recommendation for flutter prevention of curved panels whose aspect ratio is about 1 is that the panels should be able to move freely along the spanwise direction at straight edges and be tangentially restrained at curved edges. The static aerodynamic theory would provide a good prediction for flutter of such panels.

APPENDIX

Flutter speed on the occasion of panel frequency coalescence

It is well-known that a zero flutter speed may be predicted by using the static aerodynamic theory when two of the natural panel frequencies coalesce and it is a common sense that the zero critical dynamic pressure could be eliminated by inclusion of aerodynamic damping or employment of the two-dimensional quasi-steady theory or the piston theory. This is, however, not true for the flutter analysis in which an isentropic flow is assumed.

For simplicity we will consider a two-mode analysis here. According to Routh's criterion for stability, appropriate final formula on the flutter boundary is

$$\left(\frac{16}{3}Q\right)^2-2\gamma_c^2(I_{11}+I_{21})-(I_{11}-I_{21})^2=0 \quad \text{(A-1)}$$

where

$$I_{11}=I(1,1)+J_{oo}(1,1)$$
$$I_{21}=I(2,1)+J_{eo}(2,1)$$

1). When density of air is assumed constant, Eq. (19) indicates that aerodynamic damping γ_c is in proportion to a square root of dimensionless dynamic pressure Q, i.e.

$$\gamma_c=\sqrt{c_1Q} \quad \text{(A-2)}$$

Substitution of Eq. (A-2) into Eq. (A-1) yields the critical dynamic pressure

$$Q=\left(\frac{3}{16}\right)^2\left\{c_1(I_{11}+I_{21})+\sqrt{c_1^2(I_{11}+I_{21})^2+\left(\frac{16}{3}\right)^2(I_{11}-I_{21})^2}\right\} \quad \text{(A-3)}$$

If the two natural frequencies are assumed to coalesce, i.e. $I_{11}=I_{21}$, we obtain

$$Q=2\left(\frac{3}{16}\right)^2c_1(I_{11}+I_{21})\neq 0$$

This is the well-known result.

2). When a flow is assumed isentropic, substitution of Eq. (22) into Eq. (19) indicates that γ_c is proportionate to Q itself, i.e.

$$\gamma_c=\sqrt{c_2}Q \quad \text{(A-4)}$$

Equation (A-4) is substituted into Eq. (A-1) to obtain

$$Q=\frac{|I_{11}-I_{21}|}{\sqrt{\left(\frac{16}{3}\right)^2-2c_2(I_{11}+I_{21})}}$$

$$\text{for} \quad \left(\frac{16}{3}\right)^2-2c_2(I_{11}+I_{21})>0 \quad \text{(A-5)}$$

Equation (A-5) implies that the natural frequency coalescence leads to zero flutter speed in spite of inclusion of aerodynamic damping. It is also noted that we can get no flutter speed if

$$\left(\frac{16}{3}\right)^2-2c_2(I_{11}+I_{21})\leq 0$$

and that the panel does not become unstable at any dynamic pressure.

REFERENCES

1) Matsuzaki, Y., "Influence of the In-plane Boundary Conditions on the Natural Frequency of Cylindrically Curved Panels with Simply Supported Edges," *International Journal of Solids and Structures*, Vol. 7, No. 11, Nov. 1971, pp. 1555–1571.
2) Voss, H. M., "The Effect of an External Supersonic Flow on the Vibration Characteristics of Thin Cylindrical Shells," *Journal of the Aerospace Sciences*, Vol. 28, No. 12, Dec. 1961, pp. 945–956.
3) Hess, R. W. and Gibson, F. W., "Experimental Investigation of the Effects of Compressive Stress on the Flutter of a Curved Panel and a Flat Panel at Supersonic Mach Number," TN D-1386, Oct. 1962, NASA.
4) Presnell, J. G., Jr. and McKinney, R. L., "Experimental Panel Flutter Results for Some Flat and Curved Titanium Skin Panels at Supersonic Speeds," TN D-1600, Jan. 1963, NASA.
5) Bolotin, V. V., *Nonconservative Problems of the Theory of Elastic Stability*, MacMillan, New York, 1963, pp. 274–312.

6) McElman, J. A., "Flutter of Curved and Flat Sandwich Panels Subjected to Supersonic Flow," TN D-2192, April 1964, NASA.
7) Anderson, W. J. and Hsu, K-H., "Engineering Estimates for Supersonic Flutter of Curved Shell Segments," AIAA 68–284, Palm Springs, Calif., 1968.
8) Dowell, E. H., "Nonlinear Flutter of Curved Plates," *AIAA Journal*, Vol. 7, No. 3, March 1969, pp. 424–431.
9) Dowell, E. H., "Nonlinear Flutter of Curved Plates, II," *AIAA Journal*, Vol. 8, No. 2, Feb. 1970, pp. 259–261.
10) Dowell, E. H., "Panel Flutter: A Review of the Aeroelastic Stability of Plates and Shells," *AIAA Journal*, Vol. 8, No. 3, March 1970, pp. 386–399.
11) Salvioni, L., "Some Aspects of Flutter of Cylindrical Panels," *Meccanica*, Vol. 6, No. 3, Sept. 1971, pp. 139–145.
12) Reissner, E., "On Transverse Vibration of Curved Rectangular Plates," *Quarterly of Applied Mathematics*, Vol. 13, No. 2, July 1955, pp. 169–176.
13) Liepmann, H. W. and Roshko, A., *Elements of Gasdynamics*, Chap. 2, Wiley, New York, 1957.

		Yoshikazu TANABE, Kazuyuki TAKEUCHI, Koichi ONO	
TR-307	Some Characteristics of the Arc-Heater Nozzle Flow, and the Underexpanded Jet in NAL 60kW Plasma Wind Tunnel	Riichi MATSUZAKI, Noriaki HIRABAYASHI	Dec. 1972
TR-308	On the Ultrasonic Inspection in Solid Propallant Rocket Motors	Morio SHIMIZU, Yoshio NOGUCHI, Toshiharu TANEMURA	Dec. 1972
TR-309	A Numerical Calculation of a Two-Dimensional Incompressible Potential Flow Around a Set of Airfoils Applying the Relaxation Method	Masayoshi NAKAMURA	Jan. 1973
TR-310	An Evaluation of Several Difference Methods for Compresible Navier-Stokes Equations	Tomiko ISHIGURO	Mar. 1973
TR-311	On a Failure Criterion of a Solid Propellant under Triaxial Street Fields	Shuji ENDO, Kozo KAWATA	Mar. 1973
TR-312	Simulation Study on Flare Control System by Optimization Theory	Akira WATANABE, Yuso HORIKAWA	Mar. 1973
TR-313	Experimental Investigation of Two-Dimentional Cascade Performances with Blunt Trailing Edge Blade Sections at Transonic Inlet Mach Number Range	Hajime SAKAGUCHI, Hiroshi KONDO, Susumu TAKAMORI, Keigo IWASHITA	Mar. 1973
TR-314	Some Effects of Center of Gravity Locations of Added Mass on Transonic Flutter Characteristics of Low Aspect Ratio and Sweptpack Thin Cantilever Wing	Eiichi NAKAI, Moriyuki MORITA, Takao KIKUCHI, Masatoshi TOKUBO Minoru TAKAHASHI	Mar. 1973

TECHNICAL REPORT OF NATIONAL AEROSPACE LABORATORY
TR-315T

航空宇宙技術研究所報告315T号(欧文)

昭和48年4月　発行

発行所　航空宇宙技術研究所
東京都調布市深大寺町1,880
電話武蔵野三鷹(0422)47-5911(大代表)

印刷所　日新図書印刷株式会社
東京都港区芝3-33-5

Published by
NATIONAL AEROSPACE LABOLATORY
1,880 Jindaiji Chōfu, Tokyo
Japan

Printed in Japan